Chemosphere 277 (2021) 130319

Contents lists available at ScienceDirect

Chemosphere

journal homepage: www.elsevier.com/locate/chemosphere

Fate of weathered multi-walled carbon nanotubes in an aquatic sediment system

Irina Politowski [a, *], Philipp Regnery [a], Michael Patrick Hennig [a], Nina Siebers [b, c], Richard Ottermanns [a], Andreas Schäffer [a]

[a] Institute for Environmental Research, RWTH Aachen University, Worringerweg 1, 52074 Aachen, Germany
[b] Forschungszentrum Jülich GmbH, Agrosphere (IBG-3) Institute of Bio- and Geosciences, Wilhelm- Johnen-Straße, 52425, Jülich, Germany
[c] Forschungszentrum Jülich GmbH, Ernst Ruska-Centre for Microscopy and Spectroscopy with Electrons (ER-C), Wilhelm-Johnen-Straße, 52425, Jülich, Germany

HIGHLIGHTS

- Sedimentation of weathered CNT quantified at a concentration of 100 μg L^{-1}.
- Partitioning of weathered CNT in an aquatic sediment system.
- Mineralization of weathered CNT quantified using radioactive labeling.

GRAPHICAL ABSTRACT

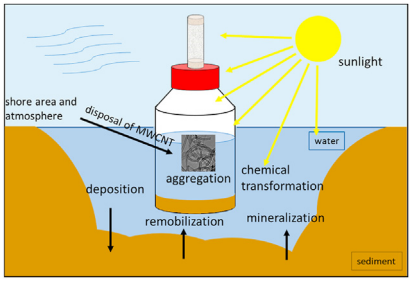

ARTICLE INFO

Article history:
Received 8 December 2020
Received in revised form
8 March 2021
Accepted 13 March 2021
Available online 16 March 2021

Handling Editor: Patryk Oleszczuk

Keywords:
Radiolabeling
Carbon nanotube
Sedimentation kinetic
Mineralization
Partitioning

ABSTRACT

The widespread application of carbon nanotubes (CNT) in various consumer products leads to their inevitable release into aquatic systems. But only little is known about their distribution among aquatic compartments. In this study, we investigated the partitioning of radiolabeled, weathered multi-walled CNT (^{14}C-wMWCNT) in an aquatic sediment system over a period of 180 days (d). The applied nanomaterial concentration in water phase was 100 μg L^{-1}. Over time, the wMWCNT disappeared exponentially from the water phase and simultaneously accumulated in the sediment phase. After 2 h incubation just 77%, after seven days 30% and after 180 d only 0.03% of applied radioactivity (AR) remained in the water phase. The respective values for the disappearance times DT_{50} and DT_{90} were 3.2 d and 10.7 d. Further, minor mineralization of ^{14}C-wMWCNT to $^{14}CO_2$ was observed with values below 0.06% of AR. In addition, a study was carried out to estimate the deposition of wMWCNT in the water phase with and without sediment in the test system for 28 d. We found no influence of a sediment phase on the sedimentation behavior of wMWCNT in the water phase: After 6.5 d and 7.3 d 50% of the applied wMWCNT subsided in the presence and absence of sediment, respectively. The slow removal of wMWCNT from the water body by deposition into sediment implies that in addition to sediment-dwelling organisms, pelagic organisms are also at risk of exposure to nanomaterials and prone for their take-up.

* Corresponding author.
E-mail address: irina.politowski@rwth-aachen.de (I. Politowski).

https://doi.org/10.1016/j.chemosphere.2021.130319
0045-6535/

1. Introduction

Carbon nanotubes (CNT) are nanoscale tubes containing only sp^2 hybridized carbon, arranged to hexagons. A distinction is made between single-walled (SWCNT) and multi-walled CNT (MWCNT), whereby the MWCNT are characterized by several tubes wound into one another. The aromatic carbon based nature of CNT gives them specific properties, such as good electrical conductivity, high tensile strength at a low density and their hydrophobic and hollow structure provides binding sites for chemical substances and pollutants (Iijima, 1991, 2002; Kennedy et al., 2008; Mauter and Elimelech, 2008). Hence, CNT are applied in the following areas: nanocomposites (Barra et al., 2019), energy storage (Wang et al., 2018), water treatment (Zaib et al., 2014; Huang et al., 2020), nanostructured fibrous scaffolds (Xia et al., 2019) and others. Comprehensive modelling of the release of CNT into the environment in Europe showed that at the end of their life cycle, nanomaterials are disposed either in landfills or in waste incineration plants (Sun et al., 2014). Since no major environmental input is expected from these handling and the entry of CNT from industrial sites is classified as very low, the predicted environmental concentration (PEC) for CNT in surface waters is estimated in the lower ng L^{-1} range (Gottschalk et al., 2009; Gottschalk and Nowack, 2011), and in sediments at least one order of magnitude higher (Gottschalk et al., 2015). Due to their advantages, an extension of CNT production is expected, which will lead to an increased release of nanomaterials to environmental compartments, both on land and in waters.

In the past, the behavior of CNT in aqueous phase has been investigated several times. It was shown that physicochemical properties of the nanomaterials, the dispersion methods and the composition of the exposure media used (ionic strength, acids, etc.) have an influence on the dispersion stability of the CNT in aqueous medium and therefore on their fate and bioavailability (Glomstad et al., 2018). In literature, accumulation of CNT in the pelagic zooplankton *Daphnia magna* and the sediment-dwelling organism *Lumbriculus variegatus* was quantified, whereas body burdens of *D. magna* decreased after 24 h of uptake, caused by the settling of CNT over time (Petersen et al., 2008, 2009, 2011a). To better understand and estimate the behavior of CNT as well as interactions between nanomaterials and biota in aquatic systems, there is a need to investigate the deposition of CNT in laboratory scale. Consequently, we performed a study on partitioning of CNT in an aqueous sediment system in accordance with OECD Guideline 308.

Further, the presence of additives such as surfactants or dissolved organic matter (DOM) in the aqueous phase can generate an electrostatic repulsion between the individual nanoparticles, which results in a reduction of agglomeration kinetics. On the other hand, a greater ionic strength leads to the suppression of the electrostatic repulsion and collision of nanoparticles results in increased agglomeration (Park et al., 2006; Hyung et al., 2007; Hyung and Kim, 2008; Saleh et al., 2008; Zhou et al., 2015). A study by Zhang et al. (2011) has also shown that DOM-MWCNT composites in aqueous solution are less susceptible to the effects of high ionic strength.

In addition, Zhang et al. (2012) showed that clay and shale minerals exhibit a binding affinity for MWCNT, which causes nanomaterials to move more rapidly from the aqueous phase to the solid phase. The above-mentioned processes either leads to an increase or a decrease of the residence time of the nanomaterials in the water phase. Especially in case of pristine nanomaterials, hydrophobic properties cause strong agglomeration processes by van der Waals forces, finally accelerating deposition to the sediment (Zhou et al., 2015; Glomstad et al., 2018). A half-live of 9 min for MWCNT (100 mg L^{-1}) and of 7.4 h for SWCNT (2.5 mg L^{-1}) was found for the deposition of CNT in water column (Kennedy et al., 2008; Schierz et al., 2014). Consequently, little is known about the deposition and partitioning considering low MWCNT concentrations. Therefore, we investigated the distribution of weathered MWCNT at lower concentrations than used in previous studies in a naturally simulated water sediment system. To track the partitioning among the different compartments we used radioactively labeled (^{14}C) CNT and developed a method to reliably quantify ^{14}C-MWCNT in sediment phase without sample combustion.

As a result of deposition and during their life cycle, CNT will end up in the sediment phase of aquatic systems. However, the distribution of CNT between water and sediment and their biodegradability is not yet well understood (Petersen et al., 2011b). The very slow mineralization and degradation of CNT by bacteria, fungi or enzymes, in part co-metabolically with an additional carbon source, has already been investigated in laboratory experiments. CNT, like black carbon (half-life of about 1400 years), are therefore among the most recalcitrant materials (Kuzyakov et al., 2009; Zhang et al., 2013; Flores-Cervantes et al., 2014; Parks et al., 2015).

Here, we aimed to study the behavior of weathered MWCNT in an aquatic sediment batch system and the distribution of the nanomaterials between aqueous and solid phase and to quantify the mineralization rate over a period of 180 days. In order to gain a better understanding of the sedimentation of MWCNT in the selected test system, the deposition of MWCNT in natural water with and without sediment phase was also examined. Sedimentation kinetics of CNT in aqueous phase are already available, but they result from studies in which high concentrations of nanomaterials were used (Kennedy et al., 2008; Schierz et al., 2014). In our study, the chosen MWCNT test concentration for both experiments was considerably lower, i.e., 100 μg L^{-1}. In surface waters, the PEC for CNT is in the ng L^{-1} range, so experiments approaching lower concentrations are necessary. Besides, the use of high CNT concentrations may lead to the erroneous results regarding the sedimentation of nanomaterials in the water column.

2. Materials and methods

2.1. Synthesis and purification of ^{14}C-labeled MWCNT (^{14}C-MWCNT)

Synthesis of ^{14}C-MWCNT has already been described elsewhere (Maes et al., 2014; Rhiem et al., 2015). Briefly, ^{14}C-MWCNT were synthesized by catalytic chemical vapour deposition. The ^{14}C label of produced ^{14}C MWCNT was located at the carbon framework. Obtained ^{14}C-MWCNT were washed using 12.5% hydrochloric acid solution to remove residues of metal catalyst, resulting in a C-purity for the product of 95%. Produced ^{14}C-MWCNT consist of 3–15 walls (4 nm for inner and 5–20 nm for outer diameter) and a length of ≥1 μm (Rhiem et al., 2015). Unlabeled MWCNT (Baytubes® C150P) were provided by Bayer Technology Services GmbH (BTS, Leverkusen, Germany) and produced under the same conditions as ^{14}C-MWCNT. The structural similarity of the nanomaterials was shown by means of transmission electron microscopy (TEM) (Rhiem et al., 2016).

2.2. Weathering of ^{14}C-MWCNT

Weathering of ^{14}C-MWCNT was performed by simulated sunlight radiation for three months (2160 h) using a weathering testing apparatus (Suntest™ CPS+, Altas Material Testing Technology, Germany, standard black temperature 65 °C, dry conditions). The device provided light with a wavelength range of 300–400 nm due to an air-cooled xenon lamp (1500 W) with a daylight UV filter.

Irradiation intensity was set to 65 W m^{-2} and the total applied energy was 505441 kJ m^{-2}. During the exposure, samples ((^{14}C) MWCNT) were placed into petri dishes with glued-on lids made of quartz glass (transmissibility for UV light). Meanwhile, the internal sample table was cooled with a constant flow of cold water. Samples were shaken once a day and the position of sample bins was changed weekly in order to achieve a uniform irradiation. After the weathering process, the specific radioactivity of ^{14}C-labeled weathered MWCNT (^{14}C-wMWCNT) was determined. Therefore, three ^{14}C-wMWCNT suspensions with 102, 186 and 488 μg of ^{14}C-wMWCNT in 102, 186 and 488 mL of deionized water, respectively, were prepared. After addition of nanomaterials, they were washed under the water surface using a pipette. Subsequently, the flask was put into an ice bath and ^{14}C-wMWCNT were dispersed by means of ultrasonication with a micro tip for 2 × 10 min (Sonopuls HD 2070, 70 W, pulse: 0.2 s, pause: 0.8 s, Bandelin, Germany) or until no more agglomerated nanomaterial was visible. Subsequently, six aliquots of 1 mL were withdrawn from each dispersion, mixed with 2 mL of Ultima Gold™ XR scintillation cocktail (PerkinElmer, Germany) and the amount of radioactivity was determined by means of LSC (liquid scintillation Analyser, Hidex 600/300 SL, Finland). Since, after homogenization, 1 μg of ^{14}C-wMWCNT was contained in 1 mL dispersion, the specific radioactivity (MBq mg^{-1}) could be calculated using the mean value of subsamples to 1.66 MBq mg^{-1}.

In order to characterize wMWCNT, thermogravimetric analysis (TGA) coupled to a Fourier-transform infrared spectrometer (FTIR) (see SI, Fig. S2) and TEM (SI, Fig. S1) methods were used. Neither differences nor heterogeneous functionalities on surface structures compared to the pristine material were detected. The observation from TGA/FTIR analysis could be based on autoxidation of the pristine MWCNT, which occurs due to prolonged storage. This is a surface functionalization depending on the surface occupancy. Other explanations could be that, e.g., COOH functionalities have decarboxylated over time and the oxidative functionalities could not be detected for this reason, or that the measurement method was not sufficiently sensitive to detect the surface modifications that have occurred. In addition, no macrostructural changes in the construction of the CNT strands could be visualized by means of TEM. Like pristine MWCNT, the weathered material showed small agglomerates and single strand exfoliated CNT after dispersion.

2.3. Sediment and water

Sediment and water used for the test system were previously collected from a local rainwater retention basin in Aachen (Germany). Sampled sediment was sieved to remove raw material (2 mm) and gently mixed to guarantee a homogeneous test mass (storage conditions: 4 °C in darkness). Natural structures and living organisms (≤2 mm) were sustained. Sediment characterization revealed a heavy silty sand (sand: 50%; silt: 47%; clay: 3%), with a total carbon content of 3.3 ± 0.1% and total organic carbon (TOC) of 2.7 ± 0.04% (Element Analyzer (CHN), elementar Analysensysteme GmbH, vario EL III, Germany), a loss on ignition of the dried sediment of 7.0 ± 0.3% and a dry weight of 45.4 ± 3.4%. To determine microbial activity in sediment, a dimethyl sulfoxide (DMSO) reduction test was performed (Alef and Kleiner, 1989). For this, sediment (1 g, air-dried for 4 h) was placed in glass vials (20 mL volume) and a DMSO solution of 5% (v/v; in water) was added. The vials were closed immediately by a gas tight screw cap with septum inlet. The test was carried out in five replicates. Samples were incubated for 24 h at 27 °C. After incubation, the produced DMS was determined by taking a sample from the vial headspace with a gas tight syringe (Hamilton, 100 μL) and subjected to GC-MS analysis (Agilent Technologies 6890 N, Software: MSD ChemStation (Agilent), Injection: 250 °C, injection in split mode (one sample in 60 s), MS: 5973 MSD, 150 °C (Agilent)). Helium was used as carrier gas (1.0 mL min^{-1}). An Optima-35MS column (Macherey und Nagel) with a length of 30.0 m and an inner diameter of 0.25 mm was used. Test was performed according to Griebler and Slezak (2001). The DMSO reduction rate is expressed as ng DMS g^{-1} dw^{-1} h^{-1}. Microbial activity of the sampled sediment was 269.4 ± 25.2 ng DMS g^{-1} dw^{-1} h^{-1}. Natural water was stored at 4 °C in closed containers and filtered using gauze (mesh size: 63 μm) before use.

2.4. Deposition of ^{14}C-wMWCNT

Deposition of CNT in water phase was tested for a^{14}C-wMWCNT concentration of 100 μg L^{-1} in the presence (+sediment) and absence (-sediment) of sediment over 28 d. Per scenario four replicates were prepared. The study was performed in 250 mL glass flasks. Prior to test start, sediment (80 mL natural sediment, see 2.3) was incubated with overlaying tap water of 5 mL for seven days to adapt the sediment to the test conditions (18 ± 1 °C, 60 rpm, darkness). In the scenario without sediment, four flasks were filled with 5 mL tap water for pre-incubation. For test start, ^{14}C-wMWCNT agglomerates were weighed on a microbalance (MYA 5.3Y, Radwag) and transferred to a flask containing 105.7 mL natural water and dispersed for 10 min as described above. Afterwards 2 × 2.5 mL of this stock dispersion was transferred to 787.5 mL natural water. The aqueous phases were again treated by means of ultrasonication tip for 10 min (see above) to obtain the test dispersions. The two-stage dispersion process as described is a deviation from the method of Rhiem et al. (2015). An investigation using TEM revealed that wMWCNT test dispersion contains small agglomerates as well as single tubes (length: 0.2 to ≥ 1 μm, see SI) and is therefore appropriate for the dispersion of wMWCNT in aqueous solution. Directly after sonication, three aliquots of 1 mL were withdrawn out of test dispersions, 2 mL of scintillation cocktail were added, and samples submitted to LSC to verify ^{14}C-wMWCNT concentration and homogeneity. Immediately after sonication, a respective volume of 175 mL out of test dispersions was applied to the prepared test systems. A concentration of 110.7 ± 3.4 μg L^{-1} and 109.2 ± 1.0 μg L^{-1} was obtained for +sediment and -sediment scenario, respectively. During application, swirling of the sediment surface was avoided as good as possible. Aliquots of 1 mL were withdrawn regularly from the top layer of water surfaces (layer depth: 0.5 cm) of all treatments and radioactivity measurement was performed as described above. Shaking was paused during sampling time (28 d), but flasks were not taken from the shaker, in order to reduce disturbance of the test systems. Decrease of radioactivity was extrapolated for the whole water body based on the taken aliquot.

2.5. Partitioning of ^{14}C-wMWCNT in an aquatic sediment system

The partitioning of ^{14}C-wMWCNT in a natural water sediment system was determined after 2 h, 1, 2, 7 and 21 days, and further after 3 and 6 months in four replicates each. Tested ^{14}C-wMWCNT concentration was 100 μg L^{-1}. The study was performed following the OECD Guideline 308 with some deviations as described hereinafter. Prior to CNT application, 250 mL flasks were filled with 80 g naturally moist sediment and covered with 5 mL tap water. Every flask was closed by a screw cap with integrated CO_2-trap containing soda lime and was incubated for 7 d (conditions: 18 ± 1 °C, 60 rpm, darkness). Additionally, two control groups (control: without nanomaterial; negative control: unlabeled wMWCNT (100 μg L^{-1})) were prepared. After acclimatization, the application of nanomaterials via the water phase was performed. Labeled and unlabeled wMWCNT were weighed on a microbalance and added to a glass flask containing 50 mL natural water, respectively. Stock

dispersions were treated by sonication for 10 min as described above. Afterwards the stock dispersions were transferred to different flasks containing natural water to gain the ^{14}C-wMWCNT test concentration and dispersed another time (10 min). Nanomaterial concentration and homogeneity of test dispersion was monitored directly after sonication (see above). The achieved ^{14}C-wMWCNT test concentration was 134.7 ± 12.3 μg L^{-1} (which corresponds to a radioactivity amount of 38.8 ± 3.7 kBq per sample). Detection limit for measurement using LSC was at 1 Bq, which corresponds to about 0.6 ng ^{14}C-wMWCNT. Therefore, and in respect to work with natural sediment, the chosen nanomaterial concentration was needed, to detect reliably nanomaterial concentration in the used matrix. Using a glass pipette, application of 175 mL stock dispersion was carried out carefully, in order to avoid disturbance of sediment surface. Each flask was capped with a screw cap with integrated CO_2-trap and incubated under the same conditions as described for pre-incubation.

2.6. Quantification of ^{14}C-wMWCNT

To quantify the formation of $^{14}CO_2$ as inorganic end product of microbial activity, soda lime pellets from CO_2 trap were dissolved in 25% hydrochloric acid solution (60–70 mL) and released $^{14}CO_2$ was absorbed by a provided scintillation cocktail (Oxysolve C-400 scintillation cocktail, Zinsser Analytic, Frankfurt a.M., Germany) in four LSC vials per replicate. After complete solution of soda lime pellets, the used equipment was flushed by nitrogen gas to collect all the developed $^{14}CO_2$. Radioactivity was measured by means of LSC. For calculation of total $^{14}CO_2$ amount per sample values from all four vials were summarized. Subsequently, removing of water phase was performed carefully using a glass pipette in order to prevent the collection of sediment particles. The water phase was filled completely into a prepared glass flask and weight was recorded. Afterwards, the water phase containing flask was placed in an ice bath and the present nanomaterials were dispersed for 10 min as described above. After homogenization, the water phase was subsampled (three aliquots of 10 g per replicate) and radioactivity was determined by means of LSC. To investigate the amount of settled CNT on the sediments surface, the water-sediment contact layer was sampled separately from the sediment. After water phase removal, the flasks were placed at a 45° angle for 15 min and the water-sediment contact layer was sampled afterwards with a Pasteur pipette and measured using LSC. To quantify the amount of ^{14}C-wMWCNT absorbed by the forming biofilm on the inner test vessel wall over time, the test vessel wall was then cleaned using a moist tissue. The tissue was mixed with 20 mL scintillation cocktail and subjected to LSC. The remaining sediment phase was dried for 24 h at 105 °C and dry weight was determined. Subsequently, the dried sediment was transferred to a ceramic mortar and grinded by hand to fine sand. To quantify the amount of ^{14}C-wMWCNT included in the sediment phase ten aliquots of ≤0.05 g per replicate were weighed in LSC vials and 0.5 mL of 35% hydrogen peroxide was added. The vials were swayed manually and incubated for 24 h at 60 °C. To suspend the sediment after drying, 0.5 mL ultrapure water was added, and the samples were gently shaken by hand. Afterwards 19.5 mL scintillation cocktail was added, and the vials were kept for 24 h in the dark at 4 °C. After cooling down, samples were acclimatized to room temperature and prior to LSC measurement, vials were placed in an ultrasonication bath and homogenized for 1 min. In a pre-test, the influence of sediment particles on quenching of flashes during LSC measurement (using an appropriate blank) was investigated (data is shown in the SI). In brief, a known amount of radioactivity (^{14}C-wMWCNT) was applied onto 20.1 ± 0.1 g sediment (dry weight), homogenized and samples were incubated at 60 °C overnight. Subsequently, the sediment was pestled and twelve aliquots of ≤0.05 g per sample were weighed into LSC vials, treated with H_2O_2 and submitted to LSC measurement. It was shown that there is no impact on efficiency of LSC measurement when particles of sediment (provided that the sample size is ≤ 0.05 g per replicate) are present in the sample. Since the recovery of ^{14}C-wMWCNT in sediment was consistent of up to 105 ± 3%, no application of a correction factor to CNT recuperation was needed.

2.7. Data evaluation and statistical analysis

Collected data were processed using Microsoft Excel® (Microsoft Office 365 ProPlus), GraphPad Prism (GraphPad Prism 5, USA), SigmaPlot (version 12.0, USA) and R (version 4.0.3, Austria). Outliers were identified by Dixon's Q test ($\alpha = 0.05$). To identify differences to zero for decreasing wMWCNT concentrations in water phase and the results for mineralization, a one-sample *t*-test (one-tailed, $\alpha = 0.05$) was performed. Raw data were tested for normality distribution with Kolmogorov-Smirnov test (p value = 0.05).

Kinetics for the sedimentation of wMWCNT (disappearance times = DT) were calculated and evaluated using Tessella Computer Assisted Kinetic Evaluation (CAKE, version 3.3). Usually this programme is intended to fit degradation kinetics of chemicals and their metabolites in line with FOCUS (FOrum for the Coordination of pesticide fate models and their USe) or NAFTA (North American Free Trade Agreement) guidelines. Regarding to the loss of ^{14}C-wMWCNT amount in a water phase as a decay like behavior, CAKE was found to be suitable. Due to the best resulting fit parameters we chose the SFO model (Single First-Order kinetics, see SI). Differences between treatments (+/− sediment) in deposition study were identified by comparing t-distributed 95% confidence intervals of slopes (k-value) from decay models.

3. Results

3.1. Deposition of ^{14}C-wMWCNT

Weathered MWCNT deposited from top layer of water surface over time. Since t-distributed 95% confidence intervals of exponent k from the applied decay model overlapped, no significant difference between +sediment (0.095–0.118) and -sediment (0.087–0.102) scenario was found (see SI, Tables S4 and S11). A more homogenous distribution of data in absence of sediment and a fluctuating course of data in presence of sediment, indicated by bigger standard deviations (e.g., on day 1, 15 and 17), was observed (Fig. 1). However, after a few days 50% of the dispersed wMWCNT have sedimented in both test systems. Sedimentation half-lives (DT_{50}) modelled by CAKE (Table 1) amounted to 6.5 d and 7.3 d in the +sediment and -sediment scenario, respectively. The applied model showed a good fit to the observed deposition data set with a coefficient of determination above 0.97 (Table 1). Nevertheless, no significant difference between the scenarios were depicted, somewhat faster sedimentation in presence of sediment is indicated by a DT_{90} of 21.7 d compared to the DT_{90} of 24.3 d in the scenario without sediment. However, in neither of the two scenarios complete sedimentation of the nanomaterials was observed within the test period. A respective residual amount of 8 ± 5% and 9 ± 2% was still detectable in the top layer of the water phase in the +sediment and -sediment approaches, respectively, even after 28 d.

3.2. Partitioning of ^{14}C-wMWCNT

The distribution of radioactivity – applied as weathered

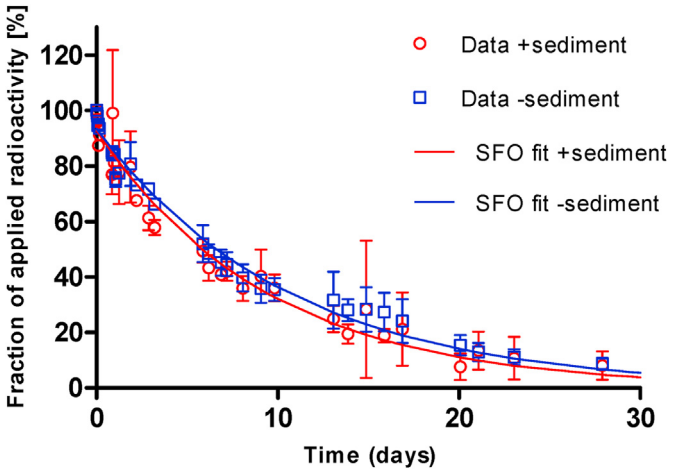

Fig. 1. Deposition of radioactively labeled multi-walled carbon nanotubes (^{14}C-wMWCNT) in a water sediment system (+sediment) and in a system containing natural water only (-sediment). A ^{14}C-wMWCNT concentration of 110.7 ± 3.4 μg L^{-1} and 109.2 ± 1.0 μg L^{-1} was applied for +sediment (A) and -sediment (B) scenario, respectively. The proportion of decrease (%) of the applied radioactivity over the test period is shown. Error bars indicate standard deviation on the mean of 4 replicates. The amount of radioactivity measured at the beginning (0 h) of the test was set to 100%. An SFO (Single First-Order) model using CAKE was fitted to the experimental data.

Table 1
Data modelling using Tessella CAKE (version 3.3) for the sedimentation of ^{14}C-wMWCNT in an aquatic sediment system over 28 days and over six months in a deposition and a partitioning study, respectively. The chosen compartment model was Single First-Order (SFO). Half-life (DT_{50}) and disappearance times after 90 days (DT_{90}) are given. Additional statistical characteristics are Chi^2 (error in %) and r^2 (observed vs. predicted data).

	Deposition study		Partitioning study
Sediment	+	−	+
Sampling	aliquots from top layer of water surface (depth: 0.5 cm)		total water compartment
DT_{50} (d)	6.5	7.3	3.2
DT_{90} (d)	21.7	24.3	10.7
Chi^2	8.4[a]	5.8[a]	16.8[a]
r^2	0.97[a]	0.98[a]	0.95[a]

[a] Denotes a non-significant lack of fit (Chi^2, 5% two-sided) and a significant slope (r, 5% one-sided).

radiolabeled MWCNT (^{14}C-wMWCNT) – among different compartments (sediment, water phase, water-sediment contact layer, mineralized amount and glass adsorbed radioactivity) in an aquatic sediment system is shown in Fig. 2. The total recovery of ^{14}C ranged between 83% and 98%. It was observed that the amount of radioactivity in the water phase decreased over time. After 2 h incubation just 77 ± 3%, after seven days 30 ± 15% and after 180 d 0.03 ± 0.01% of applied radioactivity (AR) was detected in the water phase. Therefore, a wMWCNT concentration of 0.04 μg L^{-1} remained in aqueous phase after 180 d. The suspended wMWCNT amounts in water phase after three and six months were rather low but statistically significantly different from zero (one-sample *t*-test, $\alpha = 0.05$). The respective sedimentation kinetics for DT_{50} and DT_{90} calculated by CAKE were 3.2 d and 10.7 d. The amount of radioactivity in the sediment increased over time. After 2 h of incubation, already 19 ± 4% was detected in the sediment and with termination of the study (six months), a total of 85 ± 4% of AR was found in the sediment. The more radioactivity was detected in the sediment, the lower were the recoveries (for instance: 86% after six months).

The portion of radioactivity in the water-sediment contact layer never exceeded 3% of AR and after three and six months of incubation amounted to only 0.08 ± 0.04% and 0.02 ± 0.01% of AR, respectively. Results showed that mineralization was very low, as a total of 0.02 ± 0.008%, 0.01 ± 0.003% and 0.06 ± 0.04% of AR was found after 21 d, three and six months, respectively. But statistical analysis showed that the above-mentioned amounts found for complete degradation were statistically significantly different from zero (one-sample *t*-test, $\alpha = 0.05$). Adsorption of the nanotubes to glass and the formed biofilm on the inner vessel wall was negligible, values ranged from 0.2% to 2.7% of AR. Dissolved oxygen, determined in the controls, ranged between 6.8 mg L^{-1} and 8.9 mg L^{-1} over time (75% – 97% of saturation at 20 °C) indicating water phase of the test system was oxic. The pH value in the water phases of the samples was almost constant over time and varied between 7.6 and 8.2.

4. Discussion

In the present study the deposition of 100 μg wMWCNT L^{-1} was observed in a natural water sediment system under controlled laboratory conditions. Since the 95% confidence intervals for k-values overlapped, there was no statistically significant difference in the deposition kinetics in the presence and absence of sediment (Fig. 1). We had expected that DOM introduced via the sediment would delay CNT agglomeration and discharge from the water phase, but this was not confirmed. Natural organic matter (NOM) is known to prevent agglomeration of CNT particles when present in aqueous solution, thereby increasing the dispersion stability of nanomaterials (Hyung et al., 2007). However, the sediment used consisted of 50% sand with an organic carbon content of 2.7%, which may have resulted in an insufficient amount of NOM being flushed out of the sediment and into the water phase. Contrary to our expectations the +sediment scenario showed a somewhat faster sedimentation behavior. Since the presence of sediment in the system can influence the ionic strength of the overlaying water phase, it is probable that it led to an increased sedimentation of the nanomaterials as described in the literature (Zhou et al., 2015; Glomstad et al., 2018).

The study on the partitioning of ^{14}C-wMWCNT in a water sediment system has shown that the nanomaterials are deposited into the sediment over time and thus disappeared, except for some residuals, from the water phase. Even though we were able to show in a preliminary experiment, that the amount of radioactivity in the sediment phase can be reliably detected, the recovery decreased to below 90% after an incubation period of 7 days (Fig. 2). The fact that an increasing concentration of ^{14}C-wMWCNT in the sediment phase leads to a decreasing recovery rate leads to the assumption that the nanomaterials interacted with components of the sediment (Zhang et al., 2012), which consequently reduced detectability.

However, it was shown that after a test duration of 90 days more than 99.9% of AR disappeared from the water phase (significant amounts of 0.06% after 90 d; 0.03% after 180 d remained suspended). Although it has been shown that CNT can be stabilized in the water column to a certain extent depending on the water chemistry (Zhang et al., 2011; Glomstad et al., 2018), the nanomaterials are very likely to merge with the sediment at a certain time point.

In the environment, particles in the water phase are under constant influence of water turbulence and aquatic fauna. It is conceivable that nanomaterials in raw form as well as in complexes with, e.g., DOM are ingested by organisms and excreted with the faeces (Gillis et al., 2005; Kennedy et al., 2008; Petersen et al., 2011a; Maes et al., 2014), which consequently precipitate out of the water column and become embedded in the sediment. In the

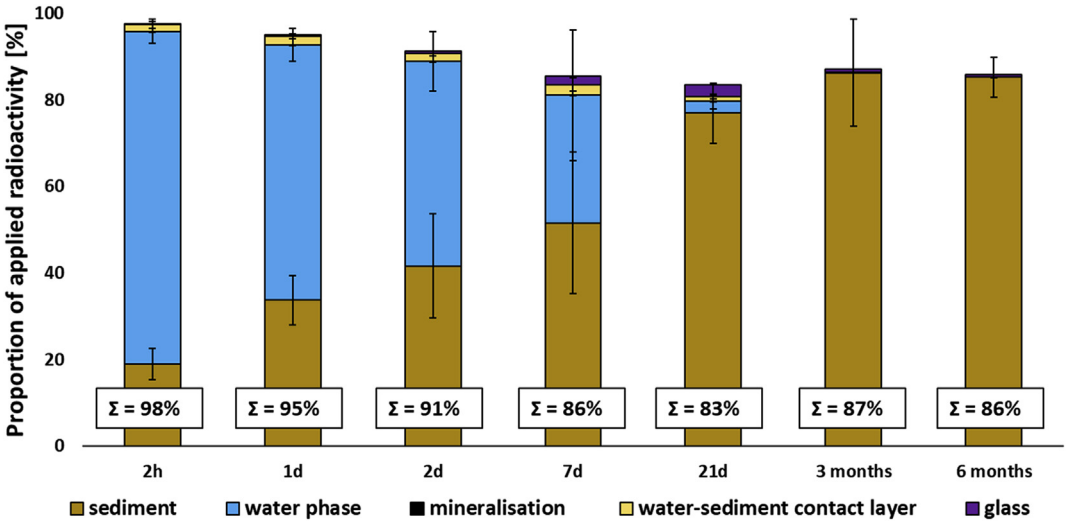

Fig. 2. Distribution of radioactivity (in % of applied radioactivity) among sediment, water phase, water-sediment contact layer, mineralized portion and radioactivity adsorbed to the used glassware over time (2 h, 1, 2, 7, 21 days, 3 and 6 months) after applying ^{14}C-wMWCNT (134.7 ± 12.3 μg L^{-1}) to an aquatic sediment system. Σ: sum of recovered radioactivity. Error bars indicate standard deviation on the mean of 4 replicates.

past, it was observed that the presence of organisms in a nanomaterial suspension promotes agglomeration of the particles and thus an increased sedimentation was observed, e.g., by passage through the gastrointestinal tract of animals, which can lead to agglutinated and insoluble agglomerates (Patra et al., 2011; Guo et al., 2013). The same was observed for coated SWCNT after intestinal passage by *Daphnia*, where the lipid layer could be reabsorbed by the organism and uncoated and clumped SWCNT were excreted (Roberts et al., 2007). On the other hand, Mao et al. (2016) showed that, during digestion excreted proteins of *Limnodrilus hoffmeisteri* coated few layer graphene (FLG) present in the water phase, which increased their solubility, leading to reduced sedimentation of FLG in the presence of *L. hoffmeisteri*.

The sediment surface represents an active interface between the aqueous and the solid phase. We showed that sedimented wMWCNT do not accumulate in the water-sediment contact layer but enter the sediment immediately after deposition, presumably due to a high binding affinity to the sediments clay mineral content of about 3% and a TOC content of 2.7%. Organic matter has aromatic ring structures as well as aliphatic molecule chains, due to π - π or CH - π interactions they tend to adsorb MWCNT (Lin and Xing, 2008; Piao et al., 2009; Zhang et al., 2012). Furthermore, it was assumed that cations and extracellular polymeric substances support bridging between CNT and NOM or within CNT particles (Zhou et al., 2015; Glomstad et al., 2018). Bouchard et al. (2017) investigated MWCNT deposition in Brier Creek (Georgia, USA) using the Water Quality Analysis Simulation Program. These studies indicated that in natural systems the disappearance of MWCNT from the upper sediment layers is triggered by burial by settling particles, resuspension and the subsequent transport of sediment particles. Therefore, it is assumed that the nanomaterials follow the same transport path as the particles to which they are attached (Bouchard et al., 2017). Subsequently, MWCNT can affect benthic organisms and microorganisms, depending on their bioavailability. Furthermore, remobilization of the sedimented CNT, e.g., by bioturbation of sediment-dwelling organisms or during flooding events, is conceivable (Bouchard et al., 2017). However, some studies found that MWCNT deposition is mostly not reversible (Chang and Bouchard, 2013; Bouchard et al., 2015; Zhao et al., 2016).

Final degradation of ^{14}C-wMWCNT to $^{14}CO_2$ was observed in the partitioning study but to a very small extent. Assuming that the mineralization kinetics is based on a linear model, the data set from six months sampling of the present study would result in a half-life of >400 years. Flores-Cervantes et al. (2014) quantified $^{14}CO_2$ evolved from a test system where ^{14}C-CNT were exposed to horseradish peroxidase and H_2O_2 and calculated half-lives of about 80 years. In addition, two further studies prove that CNT are recalcitrant substances. The co-metabolic degradation of ^{14}C-MWCNT by a bacterial community over seven days showed mineralization rates of 2%–6.8% (Zhang et al., 2013). A significantly lower mineralization rate of less than 0.1% was observed for the degradation of ^{14}C-SWCNT by the fungus *Trametes versicolor* in pure form or introduced into sediment or sludge over a period of six months (Parks et al., 2015). The values for mineralization determined in our study are thus in the lower range of the values already documented. No external microorganisms were added to our test system and the measured microbial activity in the used sediment with 269 ng DMS g^{-1} dw^{-1} h^{-1} is in the lower range compared to literature values (Lopez and Duarte, 2004).

Additionally, a weak antibacterial effect of MWCNT has been confirmed in the past so that an adverse effect on the bacterial community in the sediment cannot be excluded. (Kang et al., 2008; Baek et al., 2019). The MWCNT investigated in this study were weathered before use, but no differences in surface structure compared to pristine MWCNT were detected using TGA and FTIR (see SI). The chemical structure of carbon nanotubes suggests a high persistence of these materials. However, it is known that defects in the graphite structure, that may occur during weathering, provide vulnerabilities for degradation by microorganisms. These include vacancies in the nanotube network, open ends, sp^3 hybridizations and stone-wales defects (Yao et al., 1998; Hirsch, 2002; Niyogi et al., 2002; Tasis et al., 2006). Correspondingly, we showed that MWCNT become degraded but at a very slow rate.

The partitioning study revealed sedimentation kinetics of 3.2 d and 10.7 d (DT_{50} and DT_{90}, respectively). Although the partitioning study was conducted under the same conditions as the deposition study, the half-lives obtained differed slightly (Table 1). This difference may have been caused by the different sampling technique of the water phases. While in the deposition study only the top of the water surface was sampled, in the partitioning study the entire water phase was examined. During the sampling of the deposition

study, it was also noticed that a biological film was present on top of the water surface, which probably contained an increased amount of ^{14}C-wMWCNT and thus led to an overestimation of the wMWCNT concentration in the water phase.

In our studies, slower sedimentation kinetics compared to other studies were observed. Kennedy et al. (2008) obtained a DT_{50} of 9 min for the sedimentation of MWCNT (100 mg L^{-1}) in water containing NOM and Schierz et al. (2014) showed a DT_{50} of 7.5 h for the sedimentation of SWCNT (2.5 mg L^{-1}) in a mesocosm study. Since in both studies the water phase contained NOM, it can be assumed that the short half-lives observed in the literature are due to the initially much higher CNT concentrations used compared to the lower nanomaterial concentration applied in our study. The influence of the spiked concentration on agglomeration and stability in aqueous phase was also observed for few-layer graphene (FLG) and identified as a key factor. Within the study, Su et al. (2017) observed that the agglomeration rate of nanomaterial decreased with increasing dilution of FLG suspension. At low CNT concentrations in the water phase, as in our study, the probability of encounter and thus the frequency of agglomeration is considerably reduced, compared with concentrations in the mg L^{-1} range. The predicted environmental concentration of CNT in surface waters is in the lower ng L^{-1} range, so in general more experimental work should be performed in even lower concentration ranges. The slow sedimentation kinetics of wMWCNT clearly implies that not only sediment dwelling organisms but also those living in the water phase are exposed to engineered carbon nanomaterials.

5. Conclusion

The long residence time of CNT in the water column, ranging from several days to weeks, and their accumulation in sediment lead to the exposure of pelagic and benthic organisms. Aquatic sediment systems with different sediment and water properties as well as different types of CNT should be studied and designed to confirm our findings of long-term stability of CNT and their distribution in water sediment systems. Thus, our study and future work can contribute to a better assessment of the transport of nanomaterials in water as input parameters for modeling approaches.

Declaration of competing interest

The authors declare that they have no known competing financial interests or personal relationships that could have appeared to influence the work reported in this paper.

Acknowledgement

This work was supported by the EU Project NANO-Transfer (grant no. 03XP0061A) that receives funding from the German Federal Ministry of Education and Research (BMBF) under agreement with the FP7 ERA-NET SIINN. The responsibility for the content of this publication lies with the authors. The authors declare no financial conflict of interest. We would particularly like to thank Prof. Dr. Heinz Sturm and Dr. Ulrike Braun from BAM (German Federal Institute Materials Research and Testing) for their ambitious attempt to characterize the irradiated MWCNT. Furthermore, we want to thank Dr. Oliver Schlüter (Bayer Technology Services) for support in the synthesis of ^{14}C-labeled MWCNT. Also, we want to thank the research institute for Ecosystem Analysis and Assessment gaiac for the reliable supply of natural sediment and water and their constant assistance.

Appendix A. Supplementary data

Supplementary data to this article can be found online at https://doi.org/10.1016/j.chemosphere.2021.130319.

Credit author statement

Irina Politowski: Conzeptualization, Methodology, Investigation, Writing – original draft, Writing – review & editing. Philipp Regnery: Methodology, Investigation. Michael Patrick Hennig: Conzeptualization, Writing – original draft. Nina Siebers: Visualization, Writing – review & editing. Richard Ottermanns: Formal analysis, Writing – review & editing. Andreas Schäffer: Supervision, Project administration, Writing – review & editing

References

Alef, K., Kleiner, D., 1989. Rapid and sensitive determination of microbial activity in soils and in soil aggregates by dimethylsulfoxide reduction. Biol. Fertil. Soils 8, 349–355.
Baek, S., Joo, S.H., Su, C., Toborek, M., 2019. Antibacterial effects of graphene- and carbon-nanotube-based nanohybrids on Escherichia coli: implications for treating multidrug-resistant bacteria. J. Environ. Manag. 247, 214–223.
Barra, G., Guadagno, L., Vertuccio, L., Simonet, B., Santos, B., Zarrelli, M., Arena, M., Viscardi, M., 2019. Different methods of dispersing carbon nanotubes in epoxy resin and initial evaluation of the obtained nanocomposite as a matrix of carbon fiber reinforced laminate in terms of vibroacoustic performance and flammability. Materials 12.
Bouchard, D., Knightes, C., Chang, X., Avant, B., 2017. Simulating multiwalled carbon nanotube transport in surface water systems using the water quality analysis simulation program (WASP). Environ. Sci. Technol. 51, 11174–11184.
Bouchard, D., Chang, X., Chowdhury, I., 2015. Heteroaggregation of multiwalled carbon nanotubes with sediments. Environmental Nanotechnology, Monitoring & Management 4, 42–50.
Chang, X., Bouchard, D.C., 2013. Multiwalled carbon nanotube deposition on model environmental surfaces. Environ. Sci. Technol. 47, 10372–10380.
Flores-Cervantes, D.X., Maes, H.M., Schaffer, A., Hollender, J., Kohler, H.P., 2014. Slow biotransformation of carbon nanotubes by horseradish peroxidase. Environ. Sci. Technol. 48, 4826–4834.
Gillis, P.L., Chow-Fraser, P., Ranville, J.F., Ross, P.E., Wood, C.M., 2005. Daphnia need to be gut-cleared too: the effect of exposure to and ingestion of metal-contaminated sediment on the gut-clearance patterns of D. magna. Aquat. Toxicol. 71, 143–154.
Glomstad, B., Zindler, F., Jenssen, B.M., Booth, A.M., 2018. Dispersibility and dispersion stability of carbon nanotubes in synthetic aquatic growth media and natural freshwater. Chemosphere 201, 269–277.
Gottschalk, F., Lassen, C., Kjoelholt, J., Christensen, F., Nowack, B., 2015. Modeling flows and concentrations of nine engineered nanomaterials in the Danish environment. Int. J. Environ. Res. Publ. Health 12, 5581–5602.
Gottschalk, F., Nowack, B., 2011. The release of engineered nanomaterials to the environment. J. Environ. Monit. 13, 1145–1155.
Gottschalk, F., Sonderer, T., Scholz, R.W., Nowack, B., 2009. Modeled environmental concentrations of engineered nanomaterials (TiO(2), ZnO, Ag, CNT, Fullerenes) for different regions. Environ. Sci. Technol. 43, 9216–9222.
Griebler, C., Slezak, D., 2001. Microbial activity in aquatic environments measured by dimethyl sulfoxide reduction and intercomparison with commonly used methods. Appl. Environ. Microbiol. 67, 100–109.
Guo, X., Dong, S., Petersen, E.J., Gao, S., Huang, Q., Mao, L., 2013. Biological uptake and depuration of radio-labeled graphene by Daphnia magna. Environ. Sci. Technol. 47, 12524–12531.
Hirsch, A., 2002. Functionalization of single-walled carbon nanotubes. Angew. Chem. Int. Ed. 41, 1853–1859.
Huang, L., Li, Z., Luo, Y., Zhang, N., Qi, W., Jiang, E., Bao, J., Zhang, X., Zheng, W., An, B., He, G., 2020. Low-pressure loose GO composite membrane intercalated by CNT for effective dye/salt separation. Separ. Purif. Technol. https://doi.org/10.1016/j.seppur.2020.117839.
Hyung, H., Fortner, J.D., Hughes, J.B., Kim, J.H., 2007. Natural organic matter stabilizes carbon nanotubes in the aqueous phase. Environ. Sci. Technol. 41, 179–184.
Hyung, H., Kim, J.H., 2008. Natural organic matter (NOM) adsorption to multiwalled carbon nanotubes: effect of NOM characteristics and water quality parameters. Environ. Sci. Technol. 42, 4416–4421.
Iijima, S., 1991. Helical microtubules of graphitic carbon. Nature 354, 56–58.
Iijima, S., 2002. Carbon nanotubes: past, present, and future. Physica B 323, 1–5.
Kang, S., Herzberg, M., Rodrigues, D.F., Elimelech, M., 2008. Antibacterial effects of carbon nanotubes: size does matter! Langmuir 24, 6409–6413.
Kennedy, A.J., Hull, M.S., Steevens, J.A., Dontsova, K.M., Chappell, M.A., Gunter, J.C., Weiss Jr., C.A., 2008. Factors influencing the partitioning and toxicity of nanotubes in the aquatic environment. Environ. Toxicol. Chem. 27, 1932–1941.
Kuzyakov, Y., Subbotina, I., Chen, H., Bogomolova, I., Xu, X., 2009. Black carbon decomposition and incorporation into soil microbial biomass estimated by 14C

labeling. Soil Biol. Biochem. 41, 210–219.
Lin, D., Xing, B., 2008. Tannic acid adsorption and its role for stabilizing carbon nanotube suspensions. Environ. Sci. Technol. 42, 5917–5923.
Lopez, N.I., Duarte, C.M., 2004. Dimethyl sulfoxide (DMSO) reduction potential in mediterranean seagrass (Posidonia oceanica) sediments. J. Sea Res. 51, 11–20.
Maes, H.M., Stibany, F., Giefers, S., Daniels, B., Deutschmann, B., Baumgartner, W., Schaffer, A., 2014. Accumulation and distribution of multiwalled carbon nanotubes in zebrafish (Danio rerio). Environ. Sci. Technol. 48, 12256–12264.
Mao, L., Liu, C., Lu, K., Su, Y., Gu, C., Huang, Q., Petersen, E.J., 2016. Exposure of few layer graphene to Limnodrilus hoffmeisteri modifies the graphene and changes its bioaccumulation by other organisms. Carbon N Y 109, 566–574.
Mauter, M.S., Elimelech, M., 2008. Environmental applications of carbon-based nanomaterials. Environ. Sci. Technol. 42, 5843–5859.
Niyogi, S., Hamon, M.A., Hu, H., Zhao, B., Bhowmik, P., Sen, R., Itkis, M.E., Haddon, R.C., 2002. Chemistry of single-walled carbon nanotubes. Acc. Chem. Res. 35, 1105–1113.
Park, T.J., Banerjee, S., Hemraj-Benny, T., Wong, S.S., 2006. Purification strategies and purity visualization techniques for single-walled carbon nanotubes. J. Mater. Chem. 16, 141–154.
Parks, A.N., Chandler, G.T., Ho, K.T., Burgess, R.M., Ferguson, P.L., 2015. Environmental biodegradability of [(1)(4)C] single-walled carbon nanotubes by Trametes versicolor and natural microbial cultures found in New Bedford Harbor sediment and aerated wastewater treatment plant sludge. Environ. Toxicol. Chem. 34, 247–251.
Patra, M., Ma, X., Isaacson, C., Bouchard, D., Poynton, H., Lazorchak, J.M., Rogers, K.R., 2011. Changes in agglomeration of fullerenes during ingestion and excretion in Thamnocephalus platyurus. Environ. Toxicol. Chem. 30, 828–835.
Petersen, E.J., Pinto, R.A., Mai, D.J., Landrum, P.F., Weber Jr., W.J., 2011a. Influence of polyethyleneimine graftings of multi-walled carbon nanotubes on their accumulation and elimination by and toxicity to Daphnia magna. Environ. Sci. Technol. 45, 1133–1138.
Petersen, E.J., Zhang, L., Mattison, N.T., O'Carroll, D.M., Whelton, A.J., Uddin, N., Nguyen, T., Huang, Q., Henry, T.B., Holbrook, R.D., Chen, K.L., 2011b. Potential release pathways, environmental fate, and ecological risks of carbon nanotubes. Environ. Sci. Technol. 45, 9837–9856.
Petersen, E.J., Akkanen, J., Kukkonen, J.V., Weber Jr., W.J., 2009. Biological uptake and depuration of carbon nanotubes by Daphnia magna. Environ. Sci. Technol. 43, 2969–2975.
Petersen, E.J., Huang, Q., Weber, W.J., 2008. Ecological uptake and depuration of carbon nanotubes by Lumbriculus variegatus. Environ. Health Perspect. 116, 496–500.
Piao, L., Liu, Q., Li, Y., Wang, C., 2009. The adsorption of L-phenylalanine on oxidized single-walled carbon nanotubes. J. Nanosci. Nanotechnol. 9, 1394–1399.
Rhiem, S., Barthel, A.K., Meyer-Plath, A., Hennig, M.P., Wachtendorf, V., Sturm, H., Schaffer, A., Maes, H.M., 2016. Release of (14)C-labelled carbon nanotubes from polycarbonate composites. Environ. Pollut. 215, 356–365.
Rhiem, S., Riding, M.J., Baumgartner, W., Martin, F.L., Semple, K.T., Jones, K.C., Schaffer, A., Maes, H.M., 2015. Interactions of multiwalled carbon nanotubes with algal cells: quantification of association, visualization of uptake, and measurement of alterations in the composition of cells. Environ. Pollut. 196, 431–439.
Roberts, A.P., Mount, A.S., Seda, B., Souther, J., Qiao, R., Lin, S., Ke, P.C., Rao, A.M., Klaine, S.J., 2007. In vivo biomodification of lipid-coated carbon nanotubes by Daphnia magna. Environ. Sci. Technol. 41, 3025–3029.
Saleh, N.B., Pfefferle, L.D., Elimelech, M., 2008. Aggregation kinetics of multiwalled carbon nanotubes in aquatic systems: measurements and environmental implications. Environ. Sci. Technol. 42, 7963–7969.
Schierz, A., Espinasse, B., Wiesner, M.R., Bisesi, J.H., Sabo-Attwood, T., Ferguson, P.L., 2014. Fate of single walled carbon nanotubes in wetland ecosystems. Environ-Sci Nano 1, 574–583.
Su, Y., Yang, G.Q., Lu, K., Petersen, E.J., Mao, L., 2017. Colloidal properties and stability of aqueous suspensions of few-layer graphene: importance of graphene concentration. Environ. Pollut. 220, 469–477.
Sun, T.Y., Gottschalk, F., Hungerbuhler, K., Nowack, B., 2014. Comprehensive probabilistic modelling of environmental emissions of engineered nanomaterials. Environ. Pollut. 185, 69–76.
Tasis, D., Tagmatarchis, N., Bianco, A., Prato, M., 2006. Chemistry of carbon nanotubes. Chem. Rev. 106, 1105–1136.
Wang, J.G., Liu, H.Z., Zhang, X.Y., Li, X., Liu, X.R., Kang, F.Y., 2018. Green synthesis of hierarchically porous carbon nanotubes as advanced materials for high-efficient energy storage. Small 14.
Xia, Y., Li, S., Nie, C.X., Zhang, J.G., Zhou, S.Q., Yang, H., Li, M.J., Li, W.Z., Cheng, C., Haag, R., 2019. A multivalent polyanion-dispersed carbon nanotube toward highly bioactive nanostructured fibrous stem cell scaffolds. Appl Mater Today 16, 518–528.
Yao, N., Lordi, V., Ma, S.X.C., Dujardin, E., Krishnan, A., Treacy, M.M.J., Ebbesen, T.W., 1998. Structure and oxidation patterns of carbon nanotubes. J. Mater. Res. 13, 2432–2437.
Zaib, Q., Aina, O.D., Ahmad, F., 2014. Using multi-walled carbon nanotubes (MWNTs) for oilfield produced water treatment with environmentally acceptable endpoints. Environ Sci Process Impacts 16, 2039–2047.
Zhang, L., Petersen, E.J., Habteselassie, M.Y., Mao, L., Huang, Q., 2013. Degradation of multiwall carbon nanotubes by bacteria. Environ. Pollut. 181, 335–339.
Zhang, L., Petersen, E.J., Zhang, W., Chen, Y., Cabrera, M., Huang, Q., 2012. Interactions of 14C-labeled multi-walled carbon nanotubes with soil minerals in water. Environ. Pollut. 166, 75–81.
Zhang, L.W., Petersen, E.J., Huang, Q.G., 2011. Phase distribution of C-14-Labeled multiwalled carbon nanotubes in aqueous systems containing model solids: peat. Environ. Sci. Technol. 45, 1356–1362.
Zhao, Q., Petersen, E.J., Cornelis, G., Wang, X., Guo, X., Tao, S., Xing, B., 2016. Retention of 14C-labeled multiwall carbon nanotubes by humic acid and polymers: roles of macromolecule properties. Carbon N Y 99, 229–237.
Zhou, L., Zhu, D., Zhang, S., Pan, B., 2015. A settling curve modeling method for quantitative description of the dispersion stability of carbon nanotubes in aquatic environments. J. Environ. Sci. (China) 29, 1–10.